
Surrogate Gradients Design

Luca Herranz-Celotti Jean Rouat
Université de Sherbrooke, Canada
{luca.celotti, jean.rouat}@usherbrooke.ca

Abstract

Surrogate gradient (SG) training provides the possibility to quickly transfer all the gains made in deep learning to neuromorphic computing and neuromorphic processors, with the consequent reduction in energy consumption. Evidence supports that training can be robust to the choice of SG shape, after an extensive search of hyper-parameters. However, random or grid search of hyper-parameters becomes exponentially unfeasible as we consider more hyper-parameters. Moreover, every point in the search can itself be highly time and energy consuming for large networks and large datasets. In this article we show how complex tasks and networks are more sensitive to SG choice. Secondly, we show how low dampening, high sharpness and low tail fatness are preferred. Thirdly, we observe that *Glorot* Uniform initialization is generally preferred by most SG choices, with variability in the results. We finally provide a theoretical solution to reduce the need of extensive gridsearch, to find SG shape and initializations that result in improved accuracy.

1 Introduction

The exceptional success of deep learning comes at the cost of high energy consumption [Henderson et al., 2020]. Solving this problem is the focus of the neuromorphic research [Blouw et al., 2019; Davies et al., 2021]. The main tool in the neuromorphic arsenal is to turn deep learning neurons into spiking neurons, to encourage sparse activity, i.e., representations that are formed with many zeros and very few ones. That results in networks that can be off for the most part, with the subsequent reduction in energy consumption.

The firing process of a spiking neuron is typically defined as a non-differentiable operation for computational efficiency [Lapique, 1907; Izhikevich, 2003]. Even if biological spikes are smooth voltage curves, they are often approximated with delta functions, that are produced when the neuron voltage surpasses a threshold, then the voltage is reset to an equilibrium value. Since the neuron fires *if* the voltage is above threshold, and doesn't fire when the voltage is below the threshold, this *if* operation can be mathematically represented with a Heaviside function. However, the derivative of a Heaviside is a delta function, so a gradient that passes through a Heaviside will be zero most of the time, which makes training spiking networks with gradient descent harder. For this reason research has focused on smoothing that delta function into a shape that could pass a non-zero gradient more often [Esser et al., 2016; Zenke and Ganguli, 2018; Bellec et al., 2018]. These approximate gradients, usually referred to as surrogate gradients (SG), enable spiking networks to take advantage of the theory and practice of deep learning, backpropagation and gradient descent. Evidence suggests that training spiking networks with SG can be robust to the choice of SG shape [Zenke and Vogels, 2021], but the literature on the subject is limited and a theory of SG choice and initialization is needed.

SG training can be defined as robust if a comparable performance across SG choices is observed, after a careful hyper parameter search that depends on the SG choice. This hyper-parameter search can be highly time and energy consuming, and methods to reduce such search are of interest. If the

performance shows sizeable changes for different SG, for non carefully tuned hyper-parameters, we call SG training sensitive. In fact, different aspects of sensitivity are of interest: sensitivity to the network architecture, to the task, to the SG shape and to the initialization scheme, are some of them. We test the SG sensitivity first against more types of spiking neuron models and different tasks, to show how each network and each task has a preferred SG. We then look closely at three properties of the SG curve: its height (dampening), its width (sharpness), and its tail-fatness. This shows how successful SG training is sensitive to fine SG details. Thirdly we show that weight initialization schemes have a different impact on the final performance of each SG, which further supports the hypothesis that training is sensitive to SG choice. Therefore, a theory that allows to side step the high cost of extensive hyper-parameter search, should be easy to adapt to different architecture and task definitions, and it should be able to determine choices of dampening, sharpness, tail-fatness and initialization, that are task and network dependent.

Following the variance stability method to initialize linear and ReLU feed-forward networks proposed in [Glorot and Bengio, 2010; He et al., 2015], we construct a method for recurrent spiking networks regularization that gives conditions on initialization and SG choice, that depend on the particular network and task at hand, and can be met by tuning its dampening and its sharpness. The method controls the tendency of a network to have a variance of representation and gradient that explode or vanish exponentially with depth, and proper initialization is chosen for that purpose. In spiking recurrent networks, the Heaviside activation already keeps the forward pass activation variance from exploding exponentially, since a Bernoulli process of spiking activity can only achieve a maximal variance of $1/4$. However, the backward pass variance stability criterion provides us a method for SG choice.

Our contribution is therefore four-fold:

- we observe that complex networks and tasks are more sensitive to SG choice;
- low dampening and tail fatness, and high sharpness are preferred;
- *Glorot* Uniform initialization is generally preferred;
- we provide a method for SG choice based on bounding representations and gradients.

2 Methodology

2.1 Neural Models

Different works in the spiking neural networks literature focus on different neural models, but by far, most attention is placed on variants of the Leaky and Integrate and Fire (LIF) model [Lapique, 1907; Gerstner et al., 2014]. The Spiking Neural Unit [Woźniak et al., 2020] is essentially a pure LIF, while the Long short-term memory Spiking Neural Network [Bellec et al., 2018] is an LIF upgraded with a dynamical threshold to augment its capacity to maintain long-term memories, known as Adaptive LIF (ALIF). We propose the spiking LSTM (sLSTM), where we take the exact LSTM [Hochreiter and Schmidhuber, 1997] architecture and substitute its activations for neuromorphic activations with similar shape. We change the LSTM’s $\text{sigmoid}(x) \rightarrow \text{Heaviside}(x)$, and $\text{tanh}(x) \rightarrow 1 - 2\text{Heaviside}(x)$.

2.2 Surrogate Gradients

The Heaviside function $\tilde{H}(v)$, is defined as zero for $v < 0$ and one for $v \geq 0$. We call v the centered voltage, $v = y - \text{thr}$, where y represents the voltage of the neuron and thr the threshold. The tilde means that a surrogate gradient is used in the backward pass, defined as $\delta\tilde{H}(v) = \gamma f(s \cdot v)$, where s is the width of the surrogate gradient, also known as sharpness, γ the height or dampening factor, and f , is the shape of choice. f is chosen to have a maximal value of 1 and an area under the curve of 1. Therefore γ controls the maximal amplitude of the gradient, and s controls the width. A high sharpness, will only pass the gradient for v close to zero, while low sharpness will pass the gradient as well for a wider range of centered voltages. Notice that a SG allows the gradients to pass as well when the neuron has not fired.

The shapes f for the pseudo gradients investigated in this work are (1) a piece-wise linear triangular shape [Esser et al., 2016; Bellec et al., 2018], (2) an exponential decay [Shrestha and Orchard, 2018],

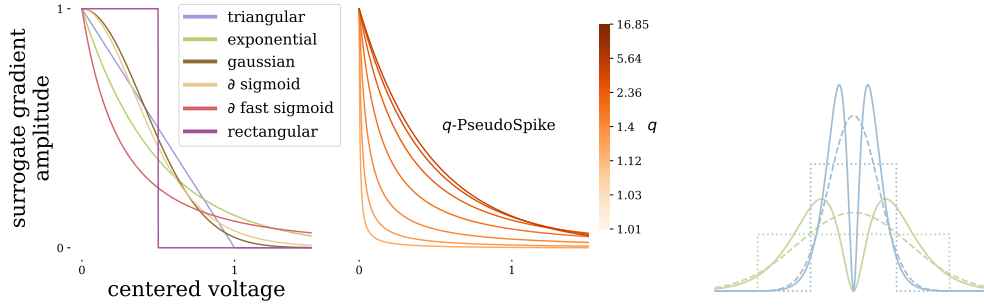


Figure 1: **Surrogate Gradient shapes and initialization distributions.** In this work we study the sensitivity of training spiking networks with gradient descent for different SG choices. Left panel shows the SG curves used throughout this study, and the tail dependence of the q -PseudoSpike SG for $q \in [1.01, 16.85]$. Right hand side shows Gaussian (dashed), Uniform (dotted) and BiGamma (solid) distributions, with *He* variance in green and *Glorot* variance in blue, for a weight shape of $(n_0, n_1) = (200, 300)$, that will be used in the analysis of the sensitivity to initialization.

(3) the derivative of a fast sigmoid, also known as SuperSpike [Zenke and Ganguli, 2018], (4) the derivative of a sigmoid, (5) a gaussian distribution and (6) a rectangular surrogate gradient, which consists of passing the derivative from the previous layer directly, only if v is smaller than $1/2$, and zero otherwise [Hubara et al., 2016]. In section 3.2 we use a generalization of the derivative of the fast sigmoid, whose tail fatness can be controlled as a hyperparameter, that we call q -PseudoSpike SG. The SG shapes can be seen in figure 1, and their equations in Appendix A.

2.3 Initialization Schemes

Proper initialization of network parameters has a strong impact on training speed [Hanin and Rolnick, 2018] and peak performance [Glorot and Bengio, 2010; He et al., 2015]. Feedforward networks are defined as $\mathbf{y}_l = b_l + W_l \sigma(\mathbf{y}_{l-1})$, where \mathbf{y}_0 is the data, \mathbf{y}_L is the output of a network of depth L , $\sigma(\cdot)$ is an activation function and $b_l \in \mathbb{R}^{n_l}$, $W_l \in \mathbb{R}^{n_{l-1} \times n_l}$ are the biases and weights of each layer, where n_l is the size of layer l . Most weight initialization schemes involve initializing biases as zero and weights such that $Mean[W_l] = 0$ and $Var[W_l] = c_l$. Theoretical work has focused on feed forward networks, and typically has found that the optimal $1/c_l$ has to be proportional to the width of the layer. The theoretical justification for this choice is that a desirable network has equally strong activity in the forward pass and gradients equally strong at each layer in the backward pass. Glorot and Bengio [2010] finds $Var[W_l] = \frac{2}{n_{l-1} + n_l}$ to be optimal for linear networks, $\sigma(x) = x$, usually referred to as *Glorot* initialization, while He et al. [2015] finds $Var[W_l] = \frac{2}{n_{l-1}}$ for *ReLU* networks, $\sigma(x) = \max(0, x)$, usually referred to as *He* initialization. Instead Saxe et al. [2014] do not find a condition on $Var[W_l]$, but find an orthogonal W_l to be optimal for mean squared error linear networks, therefore known as *Orthogonal* initialization. All the previous theoretical conditions can be accomplished with different distributions, where typically W_l elements are drawn from either a uniform or a normal distribution. We consider as well the case that we call *BiGamma* distribution, where if sampling the *Gamma* distribution we have $w_{ij} \sim \text{Gamma}(w; \alpha, \beta)$, we define the *BiGamma* as $w_{ij} \sim \text{Gamma}(w; \alpha, \beta)/2 + \text{Gamma}(-w; \alpha, \beta)/2$, shown in figure 1. Since most initialization schemes produce many weights that are equal to zero, we can understand the impact of keeping the optimal theoretical variance and orthogonality conditions with a distribution that never samples a zero.

Theoretical justification for recurrent networks initialization in the same line as the *Glorot* and *He* initializations has been proposed for the LSTM Mehdiipour Ghazi et al. [2019], where optimal constraints on the variance of the different weights are found. In the spiking networks literature, theoretical work seems to be missing, since arguments such as the Echo State [Jaeger et al., 2007], do not apply to non convex activations, or activations without a slope one regime. In practice [Zenke and Vogels, 2021] draws W_l from a uniform distribution with $Var[W_l] = \frac{1}{3n_{l-1}}$ while [Bellec et al., 2018] samples a normal distribution with $Var[W_l] = \frac{1}{n_{l-1}}$.

2.4 Datasets

Spiking Heidelberg Digits (SHD): is a dataset developed to benchmark spiking neural networks [Cramer et al., 2020]. It was created based on the Heidelberg Digits (HD) audio dataset which comprises 20 classes of spoken digits from zero to nine in English and German, spoken by 12 individuals. These audio signals are encoded into spikes through an artificial model of the inner ear and parts of the ascending auditory pathway. The train, validation and test splits have each 45k/5k/10k samples.

Spike Latency MNIST (sMNIST): the MNIST digits [LeCun et al., 1998] pixels are rescaled between zero and one, then presented as a flat vector, and each vector value is transformed into a spike timing using the transformation $T(x) = \tau_{eff} \log(\frac{x}{x-\vartheta})$ for $x > \vartheta$ and $T(x) = \infty$ otherwise, with $\vartheta = 0.2, \tau_{eff} = 50\text{ms}$ [Zenke and Vogels, 2021]. The resulting input to the network is a sequence of 50ms, of $28 \times 28 = 784$ channels, with one spike per row. The train, validation and test splits have each 8k/2k/2k samples.

PennTreeBank (PTB): is a language modelling task, chosen as a more complex alternative to classification tasks. The PennTreeBank dataset [Marcus et al., 1993], is a large corpus of American English texts with a train, validation and test splits of 930k/74k/82k words each. Next time-step prediction is performed at the word level. The one hot encoding of words can be seen as a spiking representation, even if it is the standard representation in the non neuromorphic literature.

2.5 Training Details

In all experiments we train a stack of two recurrent neural layers, where the output of the first one is fed as input to the second one, and the output of the second one is fed to the same linear readout at each time step. For the PTB task, the input passes through an embedding layer before passing to the first layer, and the output of the last layer is multiplied by the embedding to produce the output, removing the need for the readout. LIF and ALIF networks have 128 neurons per layer on the s-MNIST task, 256 on SHD, and 1300 on PTB. The sLSTM network has 64 neurons per layer on the SHD task, to keep a number of parameters comparable: 140K on SHD, 150k on sL-MNIST, 30M on PTB.

All networks have been trained with crossentropy, label smoothing of 0.1, a batch size of 32, with the AdaBelief optimizer [Zhuang et al., 2020], a learning rate of $1 \cdot 10^{-3}$, gradient norm clipped to 1, weight decay rate of 0.1, with Stochastic Weight Averaging [Izmailov et al., 2018] and Decoupled Weight Decay [Loshchilov and Hutter, 2019]. Unless explicitly stated otherwise, Glorot Uniform initialization is used. Experiments are run in single Tesla V100 NVIDIA GPUs. Each experiment is run 4 times and the mean and standard deviation are reported. The accuracy reported for classification tasks is what we call the mode accuracy: the network is required to predict the target output class at every time step, and the chosen class is taken to be the one that fired the most for the longest. In the figures, training curves show validation loss, where the validation loss was tracked during training but not used to update the weights, test loss is reported otherwise.

2.6 Theoretical LIF Initialization and SG choice

Following the approach proposed in [Glorot and Bengio, 2010; He et al., 2015] to initialize ReLU feedforward networks, we propose a method for spiking recurrent networks initialization and surrogate gradient choice. The variance stability criterion that they propose, gives us a heuristic to choose an appropriate SG.

Our discrete time LIF is going to be defined by the equation

$$\mathbf{y}_t = \alpha_{decay} \mathbf{y}_{t-1} + W_{rec} \mathbf{x}_{t-1} + \mathbf{b} + W_{in} \mathbf{z}_t - thr \mathbf{x}_{t-1} \quad (1)$$

where y_t represents the membrane voltage of the neuron, to keep the notation similar to [Glorot and Bengio, 2010; He et al., 2015], and $v_t = y_t - thr$ represents the centered voltage. We define $x_{t-1} = \sigma(y_{t-1}) = \tilde{H}(y_{t-1} - thr) = \tilde{H}(v_{t-1})$, where we use σ for a general activation, and z_t is the input at timestep t , that can come from the data, or from the neuron in the layer below in a LIF stack. It is more common to write $\alpha_{decay} = 1 - \frac{dt}{\tau_m}$, where dt is the computational time

step used, and τ_m is the membrane potential, and it is common to multiply the remaining terms by physically and biologically meaningful constants. Here we compress those constants into simpler ones, for mathematical and computational cleanliness. Each neuron can have its own speed α_{decay} , its own intrinsic current b and its own threshold thr . We present vectors in bold, e.g. \mathbf{y}_t , and their elements in light, e.g. y_t . We use upper case for matrices, e.g. W_{rec} , and lower case for their elements, e.g. w_{rec} . W_{rec} connects neurons from the same layer to each other, with zero diagonal connections, so $W_{rec} \in \mathbb{R}^{n_{rec} \times n_{rec}}$, and W_{in} connects the layer with the input, which can be another network of connected LIF or the data, so $W_{in} \in \mathbb{R}^{n_{in} \times n_{rec}}$, where n_{in} is the dimensionality of the input. We use letters or words followed by curved brackets $A(\cdot)$ to denote functions, and followed by square brackets $A[\cdot]$ to denote functionals that depend on an underlying probability distribution. When we write $\partial/\partial a$, we use a as a placeholder for any quantity that we want to propagate through gradient descent. When a stack of layers is considered, the layer definition would change to $\mathbf{y}_{t,l} = \alpha_{decay,l} \mathbf{y}_{t-1,l} + W_{rec,l} \mathbf{x}_{t-1,l} + \mathbf{b}_l + W_{in,l} \mathbf{z}_{t,l-1} - thr_l \mathbf{x}_{t,l}$, where l denotes the layer in the stack and $\mathbf{z}_{t,l-1} = \mathbf{x}_{t,l-1}$ is the activity of the layer below. Since the equation only depends on the previous time step and on the previous layer, the probability distribution will as well, making it a Markov chain in time and depth. Therefore the statistics discussed in the following, are computed element-wise with respect to the distribution $p(\mathbf{y}_{t,l}|t,l) = p(\mathbf{y}_{t-1,l}, \mathbf{z}_{t,l-1}, W_{rec,l}, W_{in,l}, \mathbf{b}_l, \alpha_{decay,l}, thr_l|t,l)$, conditioned on a given time step and layer.

We propose four conditions to initialize a stack of n_l layers of n_{rec} spiking neurons for SG training, that will give us a method to choose an SG that depends on the network and the task. We present what we consider as the mathematical equivalent after the colon:

- I each neuron has to fire half of the time: $Median[v_t] = 0$
- II recurrent and input variance should match: $Var[W_{rec}x_{t-1}] = Var[W_{in}z_t]$
- III gradients must have equal maxima across time and layers: $Max[\frac{\partial}{\partial a}y_t] = Max[\frac{\partial}{\partial a}y_{t-1}]$
- IV gradients must have equal variance across time and layers: $Var[\frac{\partial}{\partial a}y_t] = Var[\frac{\partial}{\partial a}y_{t-1}]$

The argument for condition (I) follows from the fact that SG curves are usually chosen to have non zero gradient even when the spiking neuron has not fired, but strongest when the neuron fires, shown in figure 1. Therefore, if the voltage stays close to firing, we are going to pass strong gradients more often, and that would be always the case if $Median[v] = 0$ and $Var[v] = 0$. Since $Var[v] = 0$ seems too strong as a requirement, we only assume $Median[v] = 0$ to operationalize that desiderata. The argument for condition (II) is that we want the activity to be equally sensitive to the history of presynaptic activity as it is to new input. The argument for condition (III) and (IV) is that we want gradients to be of comparable magnitude for different time steps, and for different layers in the stack, so that all the layers receive a comparable amount of information about the loss. Conditions II, III and IV are universal, in the sense that are not restricted to spiking neurons, but can be applied to any learning architecture. Condition I was introduced above to find the maxima of typical SG shape, but in general all activations in non-spiking deep learning, have their regime of interest around zero, so CI can be regarded as universal as well. Even if not explicitly stated, [Glorot and Bengio, 2010; He et al., 2015] use as well a similar condition I, $Mean[v_t] = 0$, to determine that $Mean[W_l] = Mean[b_l] = 0$ at initialization.

Therefore, the conditions as stated, are applicable to any neural network definition. When we apply the four conditions to the LIF architecture, it results in the following

$$Mean[w_{rec}] = \frac{1}{n_{rec} - 1} (3 - 2\alpha_{decay}) thr \quad \text{CI}$$

$$Var[w_{rec}] = 2(Var[z_t] + Mean[z_t]^2) \frac{n_{in}}{n_{rec} - 1} Var[w_{in}] - \frac{1}{2} Mean[w_{rec}]^2 \quad \text{CII}$$

$$\gamma = \frac{1}{(n_{rec} - 1) Min[w_{rec}] - thr Max[w_{rec}]} (1 - \alpha_{decay} - \xi n_{in} Max[w_{in}] \gamma_{in}) \quad \text{CIII}$$

$$E[\sigma'^2] = \frac{1 - \alpha_{decay}^2 - \xi n_{in} E[w_{in}^2] E[\sigma_{in}'^2]}{(n_{rec} - 1) E[w_{rec}^2] + thr^2} \quad \text{CIV}$$

and are derived in appendix B. Therefore we use the conditions to fix the values of $Mean[w_{rec}]$, $Var[w_{rec}]$, γ and s through $E[\sigma'^2]$, and the rest of the parameters that appear on the right hand side of the equations, can be chosen freely at initialization, where we assumed $b = 0$ and $Mean[w_{in}] = 0$ as desirable. The factor ξ is zero when the input comes from the data, and it is one when the input is another layer from the stack. $Var[z_t]$ and $Mean[z_t]$ are computed from the train set before training, for the first layer, while for the second we set $Mean[z_t] = 1/2$ and $Var[z_t] = 1/4$, as per Condition I. Notice that the conditions are used to fix the quantities on the left, specifically γ and s (through $E[\sigma'^2]$), which turns the conditions into tools for SG design. If the SG was fixed a priori, the conditions could be used to fix other hyper-parameters.

As shown in Appendix B.5, assuming a uniform v distribution results in a second moment for the SG of

$$E[\sigma'^2] = \frac{\gamma^2}{s(y_{max} - y_{min})} \int_{s(y_{min}-thr)}^{s(y_{max}-thr)} f(v)^2 dv \quad (2)$$

So, different SG shape f will require different sharpness s choice to meet CIV condition, since the result of the integration will depend on f . That might give an intuition on why different f could behave differently for a given choice of s . It is interesting to notice that the dependence with s is quite complex given its appearance in the integration limits, but assuming $y_{max} \rightarrow \infty$ and $y_{min} \rightarrow -\infty$, the SG variance depends quadratically with the dampening factor and inversely with the sharpness.

3 Results

3.1 Complex networks and tasks are more sensitive to SG choice

The best SG choice varies depending on the architecture (LIF, ALIF and spiking LSTM) and on the task (SHD, sl-MNIST, PTB), as shown in figure 2. The sensitivity of SG training to the architecture is shown in the upper panel, where we fix the task to be SHD and dampening and sharpness to 1. Training appears slower for the derivative of the sigmoid on LIF, but it avoids the overfitting on ALIF presented by the derivative of the fast sigmoid. We identify overfitting with the increasing validation loss curve, where the omitted training loss curve was always decreasing. Training loss curves have been omitted to avoid cluttered figures. However the derivative of the sigmoid appears to result in slow training for the sLSTM. Training with the derivative of the fast sigmoid appears to be the overall fastest but presents a tendency to overfit with ALIF towards the end, that other SG don't present. For the sLSTM, best SG seems to be the derivative of the fast sigmoid. However the sLSTM struggles to achieve a lower loss than the LIF and ALIF networks.

To evaluate SG training dependence to the task, we use the LIF network with a choice of dampening and sharpness of 1, lower panel in in figure 2. The triangular SG performs similarly to the exponential on the SHD dataset, while leads to slower training on the sl-MNIST dataset, and it does not manage to learn on the PTB dataset (covered by the rectangular SG curve). The gaussian SG is the fastest on sl-MNIST, but it performs poorly on the PTB dataset. The derivative of the fast-sigmoid systematically outperforms the rest, and the rectangular seems competitive on the SHD task, but fails training on the other.

Therefore, LIF variants are less sensitive than sLSTM to a change in SG, and classification tasks are less sensitive than language modeling tasks. Moreover, the derivative of the fast sigmoid consistently outperforms the rest.

3.2 Low dampening and tail fatness, and high sharpness are preferred

Figure 3 shows the dependency of the accuracy of the ALIF network on the sl-MNIST task for different values of dampening, sharpness and tail-fatness. When we vary the dampening or sharpness, we take the other one to be 1, which is the default value in the SG literature, and the tail is the one that corresponds to the chosen SG: $q = 2$ for the derivative of the fast sigmoid, no tail for the triangular and rectangular shapes, and exponential decays for the remaining. Low dampening is preferred by all SG choices, with an optimum at 0.8, while high levels of sharpness are preferred. Interestingly

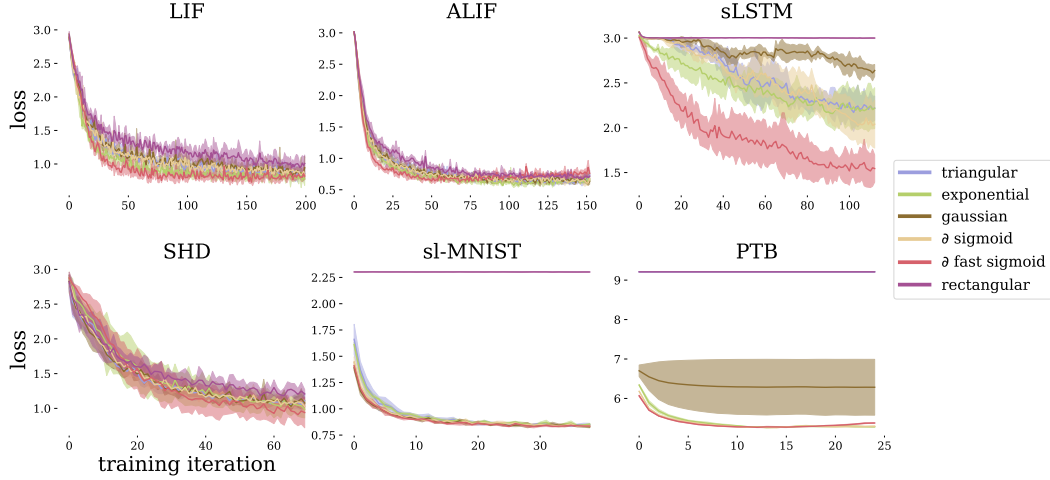


Figure 2: **Optimal SG shape, depends on the network and task.** Different aspects of the training sensitivity to SG are of interest, first and foremost, the sensitivity to the task and to the network. Upper panel shows network dependence of surrogate gradient (SG) training on the SHD task. Standard spiking neurons (LIF and ALIF) are more robust to SG choice than non standard ones (sLSTM). The best performance is achieved by the derivative of the fast sigmoid, even though it is the only one to show overfitting (identified by the increase in the validation loss with further training on the ALIF network). Lower panel shows the sensitivity of SG training to the task, on a LIF network. Triangular SG seems suboptimal but competitive on the SHD and sl-MNIST tasks, but fails training on PTB (the curve is covered by the rectangular SG, that also fails). Overall best SG is the derivative of the fast sigmoid, with a minimal overfitting on PTB.

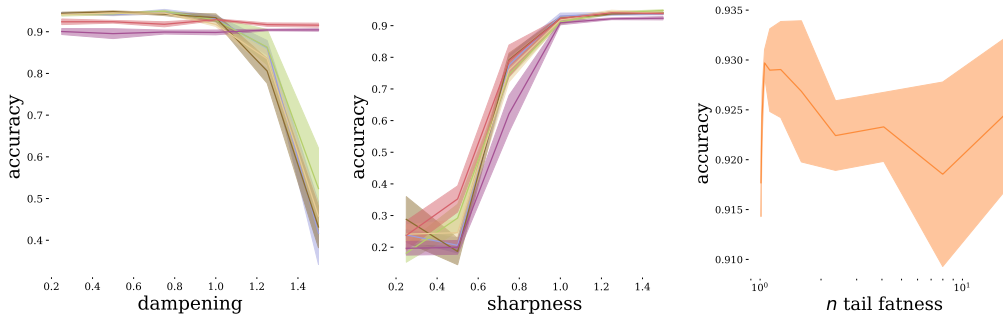


Figure 3: **SG training is sensitive to SG dampening, sharpness and tail fatness.** This sensitivity analysis is performed on the ALIF network over the sl-MNIST task. Left panel shows the sensitivity to dampening, with sharpness set to 1 and the tail fatness that characterizes the SG chosen. Center panel shows sensitivity to sharpness with a dampening of 1 and the SG tail fatness that corresponds to the SG chosen. Right panel shows sensitivity to tail fatness, for a dampening and sharpness of 1, where the tail fatness can be controlled given that the q -PseudoSpike SG used has a parameter q to control the fatness. Dampenings higher than 1 worsen performance while the pattern is the opposite for sharpness, since sharpness higher than 1 improves performance. The dependence with the tail fatness is more complex, with an optimal fatness of $q = 1.05$.

the derivative of the fast sigmoid and the rectangular SG do not lose performance with higher dampenings in the range explored, even though they are not the shapes that achieve the best accuracy for this combination of task and network. When considering the dependence with the fatness of the tail for the ALIF network on the sl-MNIST task, we fix dampening and sharpness to 1. All values for tail fatness perform reasonably well, but the exact dependence is complex, with a maximum at a tail fatness of $q = 1.05$, smaller than the $q = 2$ that would turn it into the derivative of a fast-sigmoid.

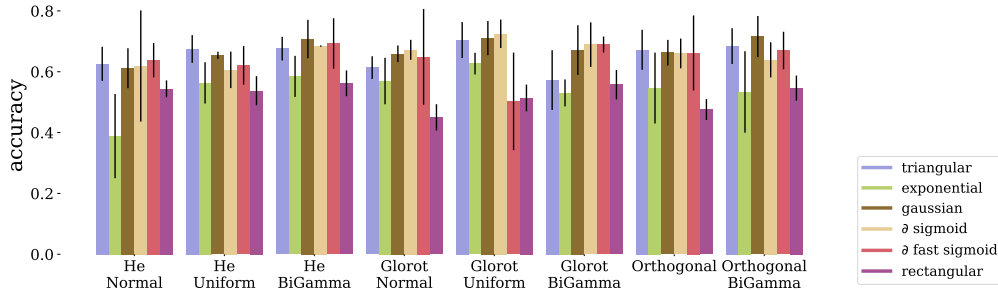


Figure 4: **SG performance ranking depends on the initialization scheme.** Means and variances are reported over 4 training seeds, when an ALIF network is trained on the SHD task. Depending on the weight initialization scheme, a different SG achieves the best accuracy. SG training is thus sensitive to the initialization scheme. Glorot Uniform prefers the derivative of a sigmoid as SG, while He Uniform prefers the triangular SG. Some SG fail completely unless the network is properly initialized, as the exponential does not achieve even a 0.4 of accuracy when the He Normal initialization is used.

3.3 Glorot Uniform is generally preferred

Figure 4 shows the sensitivity of SG training to the initialization scheme, for the ALIF network on the SHD task. We compare the *Glorot* initialization (Glorot and Bengio [2010], $2/\text{Var}[W_l] = n_{l-1} + n_l$) with *He* initialization (He et al. [2015], $2/\text{Var}[W_l] = n_{l-1}$) and *Orthogonal* initialization (Saxe et al. [2014], W_{rec} and W_{in} as orthogonal matrices). We consider 3 different sampling distributions: Uniform, Gaussian and BiGamma, see figure 1.

The best SG with Glorot Uniform initialization is the derivative of the sigmoid, while with He Normal initialization, is the derivative of the fast sigmoid. The rectangular activation improves accuracy when the weights are sampled from the BiGamma distribution. The exponential SG achieves a competitive accuracy with the Glorot Uniform initialization, but seems to fail training with the He Normal initialization. Overall best initialization scheme is *Glorot* Uniform, but leads the derivative of the fast sigmoid to worse performance than with other choices of initialization. In essence we observe that the choice of the initialization scheme goes hand in hand with the choice of SG.

3.4 Conditions I to IV improve final accuracy

Figure 5, shows the results of training after choosing initial hyper-parameters with the theoretical conditions. Results are shown for the LIF network on the SHD task, with the exponential SG. The accuracy achieved by applying the different conditions is compared with the *naive* initialization, where all weights are initialized with the *Glorot* Uniform initialization, the one that gave the best accuracy in the initialization study above. Condition II is the one to improve accuracy most when applied on its own, but the best performance is achieved when all conditions are used together. When all conditions are applied, a LIF network is able to achieve a validation accuracy of 92.7 ± 1.5 and 65.2 ± 3.1 test accuracy, compared to 87.3 ± 1.4 validation and 58.4 ± 4.9 test accuracy of the naive initialization.

4 Discussion and Conclusions

Surrogate gradients have contributed to the advance of neuromorphic computing, allowing spiking architectures to perform on par to conventional architectures, learning complex tasks with energy efficient algorithms and devices. Even if different choices of surrogate gradient shape can achieve similar performances with the correct choice of hyper parameters, to achieve systematically the best results, we have to carefully choose the best shape, for the best architecture, for a given task. This can become prohibitively expensive if a grid search of hyper-parameters has to be performed for large sets of hyper-parameters, large architectures and large datasets.

We observed that more SG shapes fail training with more complex networks and tasks. We introduced a spiking version of the LSTM, the sLSTM, but we noticed that it had remarkably poor

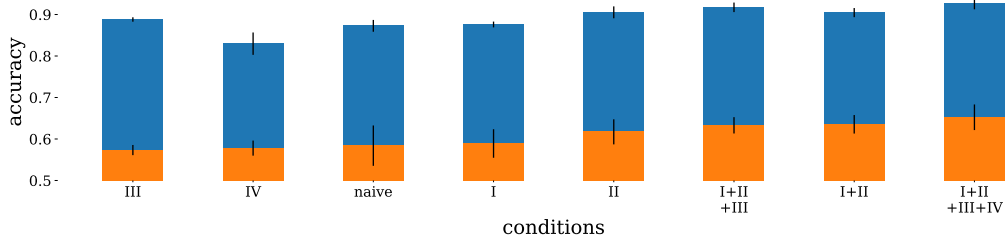


Figure 5: **Theoretically optimal initialization and SG choice.** We propose 4 theoretical initialization conditions to select an SG and improve performance of LIF networks. Condition I requires mean activity to be spiking half of the time, condition II encourages the magnitude of the network presynaptic activity to be comparable to the input current, while condition III and IV encourage the network to keep the gradient maxima and variance constant through time. The *naive* bar, corresponds to the Glorot Uniform initialization, for both W_{rec} and W_{in} , with dampening and sharpness of 1, with the exponential shape, initialization that was found experimentally to be the best choice for that SG. The experiments are run on the SHD task for an LIF network, 4 training seeds. In blue we show validation accuracy and in orange test accuracy, and conditions are ordered relative to test accuracy. Condition II has the highest impact on its own, but highest performance is achieved when all of the conditions are combined, showing a theory of initialization and SG choice can reduce the need of extensive hyper-parameter search.

performance compared to the LIF and ALIF, in contrast with the higher performance by the complete LSTM usually observed. It suggests that the LIF variants are probably already more optimal spiking architectures than previously thought. It is remarkable as well that the sLSTM seems even more sensitive to SG choice than LIF variants, and four times slower to train, suggesting that a hyper-parameter search for optimal SG training is going to be even more important for non standard spiking architectures, and so it will be a theory to avoid such a search. It is as well very interesting to notice that the PTB task, which is a language modeling task, and therefore not an arguably simpler classification task, has both triangular and rectangular SG failing training, and gaussian SG performing significantly worse, indicating that more complex tasks, might be more sensitive to SG choice.

When we focused on modifying the fine details of the SG shape, we showed that low dampening and high sharpness were preferred. We proposed the new SG shape q -PseudoSpike, that showed that the dependency with the tail is more complex, but a low tail decay of $q = 1.05$, lower than the decay of $q = 2$ of the derivative of the fast sigmoid, achieves better accuracy in our experiments. This makes the ideal surrogate shape close to a delta, with heavy tails, and therefore able to pass gradients for voltages very far from zero. On the other hand, we found the effect of the initialization scheme on SG training to be non trivial, but the *Glorot* Uniform initialization resulted often in the best accuracy for several SG shapes, in our empirical investigation. We could confirm that the derivative of the fast sigmoid, also known as SuperSpike, appears often as the best choice, followed by the exponential, that avoids some overfitting tendencies of the former. We introduced a new sampling probability for the weights, the BiGamma distribution, that is bimodal and never samples zero, and we observed that the best initialization for the derivative of the fast sigmoid was *Glorot* BiGamma.

The literature on defining optimal SG is growing in interest and activity [Nefci et al., 2019; Zenke and Vogels, 2021], but attempts to establish a theoretically optimal choice are lacking. We provide a method that can define a principled choice of dampening and sharpness, and we show mathematically the dependency of that choice with other hyper-parameters initialization, with the task and architecture, sensitivity in line with what we found numerically. We proposed as well a theory of optimal weights initialization for SG training, that is sensitive to the statistics of the task to learn. All the conditions are stated to be applicable to any spiking architecture but we derived the consequences implied on the LIF architecture. We used this theory to define the dampening and the sharpness, but conditions III and IV could be used to define a theoretical choice of tail-fatness for the q -PseudoSpike f shape instead. We showed how training under the four conditions improved accuracy over the set of hyperparameters that was found to be the best after grid search, which was *Glorot* Uniform initialization for the exponential shape. This method can therefore allow the practi-

tioner to avoid the highly time consuming task of grid search the optimal choice of hyper parameters. This is by no means the last step in the direction of optimal surrogate gradient design, and we hope this work can bring long needed clarity.

Our theory, equation 2, shows a dependence of the surrogate variance that is proportional to the square of the dampening and inversely proportional to the sharpness, which recalls our numerical findings, where a high sharpness and a low dampening were preferred, and therefore the dependency on one was inverse to the other. The theoretical conditions we propose can be easily adapted to different spiking neurons definitions, e.g. different reset methods, as we show in Appendix B.7, where the initialization equations change when a multiplicative reset with a refractory period of one time step is used in the LIF. As done in [Glorot and Bengio, 2010; He et al., 2015], this theory can be applied to convolutional W_{in} and W_{rec} , by recognizing that now $Var[W_{in}] = n_k w_{in}$ instead of $Var[W_{in}] = n_{in} w_{in}$, and analogously for the corresponding statistics of W_{rec} , where n_k is the size of the convolutional kernel, so, it is the number of presynaptic neurons a given postsynaptic neuron has.

In summary, this work replies to the call made by [Zenke and Vogels, 2021] for a theory of surrogate gradient choice, and it represents a first step in that direction.

5 Related Work

Spiking Neural Networks. Computationally, the simplest attempt to reproduce a biological neuron spiking activity is constituted by the Leaky-Integrate-and-Fire (LIF) neurons [Lapique, 1907]. When extended with an adaptive dynamic threshold, it is known to be able to reproduce qualitatively all major classes of neurons, as defined electrophysiologically in vitro [Izhikevich, 2003], and to reproduce up to 96% precision the spiking time of more complex and detailed models of neurons [Brette and Gerstner, 2005]. Non-binary spiking activity networks, such as the Spiking Neural Unit, are able to surpass LSTM in language modeling [Woźniak et al., 2020].

Surrogate Gradients. Models of biologically plausible learning rules are local [Moraitis et al., 2017; Feldman, 2020], in the sense that they involve only interchange of chemicals between a pre-synaptic and a post-synaptic neuron, and there is no straight-forward notion of a loss to be minimized, and task and architecture are not considered in the learning rule. Global signals exist, in the form of neuromodulation, but are slower [Frémaux and Gerstner, 2016; Legenstein et al., 2008; Izhikevich, 2007]. The effort to reconcile biologically plausible learning rules with gradient descent is ongoing and fruitful. One of the first successful instances of training of feed forward spiking networks with surrogate gradients was conducted by [Bohte et al., 2002], known as SpikeProp. There is no one established choice of surrogate gradients [Neftci et al., 2019], and evidence suggests that learning is robust to that choice [Zenke and Vogels, 2021]. [Bohte, 2011] have trained the network assuming no Heaviside function during training, and introduced it only at test time, while [Courbariaux et al., 2016] had the Heaviside during training, but assumed no heaviside for the backward pass. [Bellec et al., 2018] substituted the delta gradient by a triangular linearization, [Zenke and Ganguli, 2018] by the derivative of a fast sigmoid, and [Zenke and Vogels, 2021] by the derivative of a sigmoid.

6 Acknowledgements

Luca Herranz-Celotti was supported by the Natural Sciences and Engineering Research Council of Canada through the Discovery Grant from professor Jean Rouat. We thank Compute Canada for the clusters used to perform the experiments and NVIDIA for the donation of two GPUs. We thank Wolfgang Maass for the possibility to visit their lab, Guillaume Bellec, Darjan Salaj and Franz Scherr, for their invaluable insights on learning with surrogate gradients, and Maryam Hosseini for her feedback on the current draft.

References

S. Basu and A. DasGupta. The mean, median, and mode of unimodal distributions: a characterization. *Theory of Probability & Its Applications*, 41(2):210–223, 1997.

- G. Bellec, D. Salaj, A. Subramoney, R. Legenstein, and W. Maass. Long short-term memory and learning-to-learn in networks of spiking neurons. In *Advances in Neural Information Processing Systems*, 2018.
- P. Blouw, X. Choo, E. Hunsberger, and C. Eliasmith. Benchmarking keyword spotting efficiency on neuromorphic hardware. In *Proceedings of the 7th Annual Neuro-inspired Computational Elements Workshop*, pages 1–8, 2019.
- S. M. Bohte. Error-backpropagation in networks of fractionally predictive spiking neurons. In T. Honkela, W. Duch, M. Girolami, and S. Kaski, editors, *Artificial Neural Networks and Machine Learning – ICANN 2011*, pages 60–68, Berlin, Heidelberg, 2011. Springer Berlin Heidelberg. ISBN 978-3-642-21735-7.
- S. M. Bohte, J. N. Kok, and H. La Poutre. Error-backpropagation in temporally encoded networks of spiking neurons. *Neurocomputing*, 48(1-4):17–37, 2002.
- R. Brette and W. Gerstner. Adaptive exponential integrate-and-fire model as an effective description of neuronal activity. *Journal of neurophysiology*, 94(5):3637–3642, 2005.
- M. Courbariaux, I. Hubara, D. Soudry, R. El-Yaniv, and Y. Bengio. Binarized neural networks: Training deep neural networks with weights and activations constrained to+ 1 or-1. *arXiv preprint arXiv:1602.02830*, 2016.
- B. Cramer, Y. Stradmann, J. Schemmel, and F. Zenke. The heidelberg spiking data sets for the systematic evaluation of spiking neural networks. *IEEE Transactions on Neural Networks and Learning Systems*, 2020.
- M. Davies, A. Wild, G. Orchard, Y. Sandamirskaya, G. A. F. Guerra, P. Joshi, P. Plank, and S. R. Risbud. Advancing neuromorphic computing with loihi: A survey of results and outlook. *Proceedings of the IEEE*, 109(5):911–934, 2021. doi: 10.1109/JPROC.2021.3067593.
- S. K. Esser, P. A. Merolla, J. V. Arthur, A. S. Cassidy, R. Appuswamy, A. Andreopoulos, D. J. Berg, J. L. McKinstry, T. Melano, D. R. Barch, et al. Convolutional networks for fast, energy-efficient neuromorphic computing. *Proceedings of the national academy of sciences*, 113(41): 11441–11446, 2016.
- D. E. Feldman. Chapter 6 - spike timing-dependent plasticity. In J. Rubenstein, P. Rakic, B. Chen, and K. Y. Kwan, editors, *Neural Circuit and Cognitive Development (Second Edition)*, pages 127–141. Academic Press, second edition, 2020. ISBN 978-0-12-814411-4. doi: <https://doi.org/10.1016/B978-0-12-814411-4.00006-8>.
- N. Frémaux and W. Gerstner. Neuromodulated spike-timing-dependent plasticity, and theory of three-factor learning rules. *Frontiers in neural circuits*, 9:85, 2016.
- W. Gerstner, W. M. Kistler, R. Naud, and L. Paninski. *Neuronal dynamics: From single neurons to networks and models of cognition*. Cambridge University Press, 2014.
- X. Glorot and Y. Bengio. Understanding the difficulty of training deep feedforward neural networks. In *Proceedings of the thirteenth international conference on artificial intelligence and statistics*, pages 249–256. JMLR Workshop and Conference Proceedings, 2010.
- B. Hanin and D. Rolnick. How to start training: The effect of initialization and architecture. In *NeurIPS*, 2018.
- K. He, X. Zhang, S. Ren, and J. Sun. Delving deep into rectifiers: Surpassing human-level performance on imagenet classification. In *Proceedings of the IEEE international conference on computer vision*, pages 1026–1034, 2015.
- P. Henderson, J. Hu, J. Romoff, E. Brunskill, D. Jurafsky, and J. Pineau. Towards the systematic reporting of the energy and carbon footprints of machine learning. *Journal of Machine Learning Research*, 21(248):1–43, 2020.
- S. Hochreiter and J. Schmidhuber. Long short-term memory. *Neural computation*, 9(8):1735–1780, 1997.

- I. Hubara, M. Courbariaux, D. Soudry, R. El-Yaniv, and Y. Bengio. Binarized neural networks. *Advances in neural information processing systems*, 29, 2016.
- E. M. Izhikevich. Simple model of spiking neurons. *IEEE Transactions on neural networks*, 14(6):1569–1572, 2003.
- E. M. Izhikevich. Solving the distal reward problem through linkage of stdp and dopamine signaling. *Cerebral cortex*, 17(10):2443–2452, 2007.
- P. Izmailov, D. Podoprikin, T. Garipov, D. Vetrov, and A. Wilson. Averaging weights leads to wider optima and better generalization. In R. Silva, A. Globerson, and A. Globerson, editors, *34th Conference on Uncertainty in Artificial Intelligence 2018, UAI 2018*, 34th Conference on Uncertainty in Artificial Intelligence 2018, UAI 2018, pages 876–885. Association For Uncertainty in Artificial Intelligence (AUAI), 2018.
- H. Jaeger, M. Lukoševičius, D. Popovici, and U. Siewert. Optimization and applications of echo state networks with leaky-integrator neurons. *Neural networks*, 20(3):335–352, 2007.
- L. Lapique. Recherches quantitatives sur l’excitation électrique des nerfs traitée comme une polarisation. *Journal of Physiology and Pathology*, 9:620–635, 1907.
- Y. LeCun, L. Bottou, Y. Bengio, and P. Haffner. Gradient-based learning applied to document recognition. *Proceedings of the IEEE*, 86(11):2278–2324, 1998.
- R. Legenstein, D. Pecevski, and W. Maass. A learning theory for reward-modulated spike-timing-dependent plasticity with application to biofeedback. *PLoS computational biology*, 4(10):e1000180, 2008.
- I. Loshchilov and F. Hutter. Decoupled weight decay regularization. In *International Conference on Learning Representations*, 2019.
- M. P. Marcus, B. Santorini, and M. A. Marcinkiewicz. Building a large annotated corpus of English: The Penn Treebank. *Computational Linguistics*, 19(2):313–330, 1993.
- M. Mehdipour Ghazi, M. Nielsen, A. Pai, M. Modat, M. Cardoso, S. Ourselin, and L. Sørensen. On the initialization of long short-term memory networks. In T. Gedeon, K. Wong, and M. Lee, editors, *Neural Information Processing - 26th International Conference, ICONIP 2019, Proceedings*, Lecture Notes in Computer Science (including subseries Lecture Notes in Artificial Intelligence and Lecture Notes in Bioinformatics), pages 275–286. Springer VS, 2019. ISBN 9783030367077. doi: 10.1007/978-3-030-36708-4_23. 26th International Conference on Neural Information Processing, ICONIP 2019 ; Conference date: 12-12-2019 Through 15-12-2019.
- T. Moraitis, A. Sebastian, I. Boybat, M. Le Gallo, T. Tuma, and E. Eleftheriou. Fatiguing stdp: Learning from spike-timing codes in the presence of rate codes. In *2017 International Joint Conference on Neural Networks (IJCNN)*, pages 1823–1830, 2017. doi: 10.1109/IJCNN.2017.7966072.
- E. O. Neftci, H. Mostafa, and F. Zenke. Surrogate gradient learning in spiking neural networks: Bringing the power of gradient-based optimization to spiking neural networks. *IEEE Signal Processing Magazine*, 36(6):51–63, 2019. doi: 10.1109/MSP.2019.2931595.
- A. M. Saxe, J. L. McClelland, and S. Ganguli. Exact solutions to the nonlinear dynamics of learning in deep linear neural networks. In Y. Bengio and Y. LeCun, editors, *2nd International Conference on Learning Representations, ICLR 2014, Banff, AB, Canada, April 14-16, 2014, Conference Track Proceedings*, 2014.
- S. Shrestha and G. Orchard. Slayer: Spike layer error reassignment in time. In *NeurIPS*, 2018.
- S. Woźniak, A. Pantazi, T. Bohnstingl, and E. Eleftheriou. Deep learning incorporating biologically inspired neural dynamics and in-memory computing. *Nature Machine Intelligence*, 2(6):325–336, 2020.
- F. Zenke and S. Ganguli. Superspike: Supervised learning in multilayer spiking neural networks. *Neural computation*, 30(6):1514–1541, 2018.

- F. Zenke and T. P. Vogels. The remarkable robustness of surrogate gradient learning for instilling complex function in spiking neural networks. *Neural Computation*, 33(4):899–925, 2021.
- J. Zhuang, T. Tang, Y. Ding, S. C. Tatikonda, N. Dvornek, X. Papademetris, and J. Duncan. Ad-abelief optimizer: Adapting stepsizes by the belief in observed gradients. *Advances in Neural Information Processing Systems*, 33, 2020.

1 Supplementary Material

A List of Surrogate Gradients shapes

We list here the shapes that we used in this article as surrogate gradient.

$f(v)$		
	triangular	$\max(1 - v , 0)$
	exponential	$e^{-2 v }$
	gaussian	$e^{-\pi v^2}$
	∂ sigmoid	$4 \text{sigmoid}(4v) (1 - \text{sigmoid}(4v))$
	∂ fast-sigmoid	$\frac{1}{(1+ 2v)^2}$
	rectangular	$\mathbb{1}_{ v < \frac{1}{2}}$
	q-PseudoSpike ($q > 1$)	$\frac{1}{(1+\frac{2}{q-1} v)^q}$

Table S1: Here we show the mathematical definition of the surrogate gradients studied in this article. Our Heaviside activation $\tilde{H}(v)$, where v is the centered voltage, has the surrogate gradient $\delta\tilde{H}(v) = \gamma f(s \cdot v)$, where s is the sharpness of the surrogate gradient, or its width, γ the dampening factor, or its height, and f is the shape of choice. Its constants, are chosen for it to have a maximal value of 1 and an area under the curve of 1.

B Detailed derivation of the conditions

We would be pleased to get feedback, suggestions and potential corrections about the following developments. Please read considering that we are still reviewing the correctness of the calculations.

B.1 Impact of centered voltage constraint on the connectivity (Condition I)

We show how the use of condition I leads to a constraint on how to initialize the network connectivity with an LIF neuron model, that will lead the network to meet that condition at initialization.

Our LIF network is defined by

$$\mathbf{y}_t = \alpha_{decay} \mathbf{y}_{t-1} + W_{rec} \mathbf{x}_{t-1} + W_{in} \mathbf{z}_t + \mathbf{b} - thr \mathbf{x}_{t-1} \quad (3)$$

First we show that $Median[v] = 0 \implies Mean[x] = 1/2$, where $x = \tilde{H}(v)$. Detailed textual description follows the mathematical analysis. We have

$$Mean[x] = \int xp(x)dx \quad (4)$$

$$= \int xp(x|v)p(v)dx dv \quad (5)$$

$$= \int xp(v)\delta(x - H(v))dx dv \quad (6)$$

$$= \int p(v)dvH(v) \quad (7)$$

$$= \int_0^\infty p(v)dv \quad (8)$$

In equation 5 we write the marginal distribution of $p(x) = \int p(x|v)p(v)dv$, and the double integral is represented with one integration symbol. In the following equation we notice that x does not depend probabilistically with v , but it is a deterministic dependence, since it is a function we know, $x = H(v)$, distribution that we represent with the delta function $p(x|v) = \delta(x - H(v))$. Then we integrate over x , and in the last equation we notice that integrating wrt the Heaviside is like restricting the integration limits from zero to infinity. If $Median[v] = 0$, half of its probability mass is on each side of 0, so the last integral is equal to 1/2, QED.

Since working with medians is mathematically harder than working with means, we assume that $Mean[v] \approx Median[v]$, with the caveat that it will make the result approximate. To justify that they are similar, it can be shown that for a unimodal distribution $v \sim p(v)$ with the first two moments defined, we have $|Mean[v] - Median[v]| \leq \sqrt{0.6Var[v]}$ [Basu and DasGupta, 1997]. We will proceed with this approximation in mind, and we will continue the development with means and not with medians.

We will use $\mathbf{y}_t = \alpha_{decay} \mathbf{y}_{t-1} + \mathbf{i}_t$ for brevity, where $\mathbf{i}_t = W_{rec} \mathbf{x}_{t-1} + W_{in} \mathbf{z}_t + \mathbf{b} - thr \mathbf{x}_{t-1}$. If we calculate how the mean of its elements is propagated through time

$$Mean[\mathbf{y}_t] = Mean[\alpha_{decay}]Mean[\mathbf{y}_{t-1}] + Mean[\mathbf{i}] \quad (9)$$

$$= Mean[\alpha_{decay}] \left(Mean[\alpha_{decay}]Mean[\mathbf{y}_{t-2}] + Mean[\mathbf{i}] \right) + Mean[\mathbf{i}] \quad (10)$$

$$= Mean[\alpha_{decay}]^{t-1} Mean[\mathbf{y}_1] + \left(\sum_{t'=0}^{t-2} Mean[\alpha_{decay}]^{t'} \right) Mean[\mathbf{i}] \quad (11)$$

$$= Mean[\alpha_{decay}]^{t-1} Mean[\mathbf{y}_1] + \frac{1 - Mean[\alpha_{decay}]^{t-1}}{1 - Mean[\alpha_{decay}]} Mean[\mathbf{i}] \quad (12)$$

where we used the fact that the same LIF definition applies to different time steps, the geometric series formula, and the fact that for independent random variables $E[XY] = E[X]E[Y]$. We assumed the mean input current to remain constant over time $Mean[i_t] = Mean[i]$, to simplify the mathematical development. For $t \rightarrow \infty$ and using the fact that $0 < Mean[\alpha_{decay}] < 1$

$$Mean[y_t] = \frac{1}{1 - Mean[\alpha_{decay}]} Mean[i] \quad (13)$$

$$Mean[y_t] - Mean[thr] = \frac{1}{1 - Mean[\alpha_{decay}]} Mean[i] - Mean[thr] \quad (14)$$

Assuming we want this condition to hold independently of the dataset, we set $Mean[W_{in}] = 0$, and assuming that we do not want to promote this behavior with fixed internal currents, but with the recurrent activity instead, then $\mathbf{b} = 0$.

We remark that we denote $Mean[W\mathbf{x}]$ as the mean vector whose element i is

$$Mean[W\mathbf{x}]_i = Mean\left[\sum_{\substack{j=1 \\ j \neq i}} w_{ij}x_j\right] = \sum_{\substack{j=1 \\ j \neq i}} Mean[w_{ij}x_j] = \sum_{\substack{j=1 \\ j \neq i}} Mean[w]x_j = (n_{rec} - 1)Mean[w]x_i \quad (15)$$

where the condition $j \neq i$ in the summand reminds that neurons are not connected to themselves in our recurrent architecture. In the first equality, the index i denoting the element in the vector, is equivalent as choosing the row i of W , so it is not necessary to specify it outside the square brackets. The equality before the last one is a consequence of considering any neuron as mutually independent to any other at initialization, as done by [Glorot and Bengio, 2010; He et al., 2015], and that justifies dropping the indices. Since w and x are statistically independent random variables, $Mean[w]x_i = Mean[w]Mean[x_i]$.

Then,

$$Mean[y_t - thr] = \frac{1}{1 - Mean[\alpha_{decay}]} ((n_{rec} - 1)Mean[w_{rec}]Mean[x_{t-1}] - Mean[thr]Mean[x_{t-1}]) - Mean[thr] \quad (16)$$

$$0 = \frac{1}{1 - Mean[\alpha_{decay}]} ((n_{rec} - 1)Mean[w_{rec}]Mean[x_{t-1}] - Mean[thr]Mean[x_{t-1}]) - Mean[thr] \quad (17)$$

$$0 = \frac{Mean[x_{t-1}]}{1 - Mean[\alpha_{decay}]} ((n_{rec} - 1)Mean[w_{rec}] - Mean[thr]) - Mean[thr] \quad (18)$$

$$Mean[w_{rec}] = \frac{1}{(n_{rec} - 1)} \frac{1 - Mean[\alpha_{decay}]}{Mean[x_{t-1}]} Mean[thr] + Mean[thr] \quad (19)$$

$$Mean[w_{rec}] = \frac{1}{(n_{rec} - 1)} (3 - 2Mean[\alpha_{decay}]) Mean[thr] \quad (20)$$

where in the second line we applied condition I in the form of $Mean[v_t] \approx Median[v_t] = 0$, so $Mean[y_t - thr] = 0$, and in the last step we applied again condition I, $Mean[x_t] = 1/2$. In the main text we turn $Mean[thr], Mean[\alpha_{decay}] \rightarrow thr, \alpha_{decay}$, since here we consider the more general case where those are as well random variables, and we simplify it in the main text for cleanliness, assuming they are constant.

We therefore found a constraint on the recurrent matrix initialization, that leads the LIF network to satisfy condition I at initialization.

B.2 Impact on the connectivity of the equal contribution from recurrency and input to the voltage variance (Condition II)

We apply the condition II to the LIF network, that gives us a constraint that the recurrent matrix has to meet at initialization for the condition to be true. The second condition, is that the recurrent and the input contribution to the variance has to match

$$\text{Var}[W_{rec}x_{t-1}] = \text{Var}[W_{in}z_t] \quad (21)$$

where the variance is computed at each element, after the matrix multiplication is performed, following the method described in [Glorot and Bengio, 2010; He et al., 2015]. Similarly to what we did for the means in equation 15, the matrix multiplication contributes to the scalar variance of neuron i as

$$\text{Var}[W\mathbf{x}]_i = \text{Var}\left[\sum_{j=1} w_{ij}x_j\right] = \sum_{j=1} \text{Var}[w_{ij}x_j] = \sum_{j=1} \text{Var}[wx] = n_W \text{Var}[wx] \quad (22)$$

The second and third equality are a consequence of considering any neuron as mutually independent to any other at initialization, as done by [Glorot and Bengio, 2010; He et al., 2015], and that justifies that the variance of the sum is the sum of the variances, and it justifies dropping the indices, to mean that the statistics are the same for each element. The number n_W stands for the number of inputs that a neuron i has through W , in the case of W_{in} , $n_W = n_{in}$, while in the case of W_{rec} , we have $n_W = n_{rec} - 1$, since in our recurrent network, neurons are not connected to themselves.

Therefore the vector-wise condition II is equivalent to the element-wise

$$(n_{rec} - 1)\text{Var}[w_{rec}x_{t-1}] = n_{in}\text{Var}[w_{in}z_t] \quad (23)$$

We consider as well that a network that fires $E[x_t] = p$, has $\text{Var}[x_t] = p(1 - p)$ when averaged over time, since when the time dimension is averaged out, the time axis can be randomly shuffled, and the LIF activity is indistinguishable from a Bernoulli process through that statistic.

We apply the fact that for independent w, x

$$\text{Var}[wx] = (\text{Var}[x] + E[x]^2)(\text{Var}[w] + E[w]^2) - E[x]^2 E[w]^2 \quad (24)$$

and assuming $E[w_{in}] = 0$ and $p = 1/2$ we have

$$\text{Var}[w_{rec}x_{t-1}] = p(\text{Var}[w_{rec}] + \text{Mean}[w_{rec}]^2) - p^2 \text{Mean}[w_{rec}]^2 = \frac{1}{4}(2\text{Var}[w_{rec}] + \text{Mean}[w_{rec}]^2) \quad (25)$$

$$\text{Var}[w_{in}z_t] = (\text{Var}[z_t] + \text{Mean}[z_t]^2)\text{Var}[w_{in}] \quad (26)$$

Substituting in equation 23 implies

$$\frac{1}{4}(2\text{Var}[w_{rec}] + \text{Mean}[w_{rec}]^2) = (\text{Var}[z_t] + \text{Mean}[z_t]^2) \frac{n_{in}}{n_{rec} - 1} \text{Var}[w_{in}] \quad (27)$$

$$\text{Var}[w_{rec}] = 2(\text{Var}[z_t] + \text{Mean}[z_t]^2) \frac{n_{in}}{n_{rec} - 1} \text{Var}[w_{in}] - \frac{1}{2} \text{Mean}[w_{rec}]^2 \quad (28)$$

Therefore condition II led us to the constraint that W_{rec} has to meet at initialization for the condition to be true. The final equation further assumes that $E[w_{in}] = 0$ and $p = 1/2$.

B.3 Impact on the SG dampening of the gradient maximums stability through time (Condition III)

We want the maximal value of the gradient to remain stable, without exploding, when transmitted through time and through different layers

$$Max[\frac{\partial}{\partial a}y_t] = Max[\frac{\partial}{\partial a}y_{t-1}] \quad (29)$$

where when we write $\partial/\partial a$, we use a as a placeholder for any quantity that we want to propagate through gradient descent. Taking the derivative of the LIF definition we have

$$\frac{\partial}{\partial a}y_t = \alpha_{decay} \frac{\partial}{\partial a}y_{t-1} + W_{rec} \frac{\partial}{\partial a}x_{t-1} + \xi W_{in} \frac{\partial}{\partial a}z_t - thr \frac{\partial}{\partial a}x_{t-1} \quad (30)$$

Here we introduce the symbol $\xi \in \{0, 1\}$, to keep the possibility of the gradient having to pass through z_t to reach the layer below, $\xi = 1$, and the possibility of z_t being instead the data, removing the need to pass the gradient, $\xi = 0$. We consider as well that

$$\frac{\partial}{\partial a}z_t = \frac{\partial}{\partial a}\tilde{H}_{in}(y_t^{in} - thr_{in}) = \sigma'_{in} \frac{\partial}{\partial a}y_t^{in} \quad (31)$$

$$\frac{\partial}{\partial a}x_{t-1} = \frac{\partial}{\partial a}\tilde{H}(y_{t-1} - thr) = \sigma' \frac{\partial}{\partial a}y_{t-1} \quad (32)$$

where $\tilde{H}_{in}, y_t^{in}, thr_{in}$ are the surrogate step-function, the voltage at time t and the threshold of the layer below and $\sigma' = \frac{\partial \tilde{H}}{\partial v}$ is the surrogate gradient, and σ'_{in} is the surrogate gradient from the level below. Substituting in equation 30, it results in

$$\frac{\partial}{\partial a}y_t = \alpha_{decay} \frac{\partial}{\partial a}y_{t-1} + W_{rec} \sigma' \frac{\partial}{\partial a}y_{t-1} + \xi W_{in} \sigma'_{in} \frac{\partial}{\partial a}y_t^{in} - thr \sigma' \frac{\partial}{\partial a}y_{t-1} \quad (33)$$

We use Max and Min in a statistical ensemble sense, as the maximum/minimum value that a variable could take if sampled over and over again

$$Max[X] = \sup_{x \sim p(x)} x \quad (34)$$

$$Min[X] = \inf_{x \sim p(x)} x \quad (35)$$

With this definition, if X, Y are independent random variables $Max[X+Y] = Max[X] + Max[Y]$ and if they are positive $Max[XY] = Max[X]Max[Y]$. We observe, as we did before for the variance and the mean of Wx , that

$$Max[Wx] = n_W Max[wx] \quad (36)$$

$$Min[Wx] = n_W Min[wx] \quad (37)$$

Taking the maximal value of $\frac{\partial}{\partial a}y_t$, and making the strong assumption that $\sigma', \frac{\partial}{\partial a}y_{t-1}$ are statistically independent

$$\text{Max}\left[\frac{\partial}{\partial a}y_t\right] = \text{Max}\left[\alpha_{decay}\frac{\partial}{\partial a}y_{t-1}\right] + (n_{rec} - 1)\text{Max}\left[w_{rec}\sigma'\frac{\partial}{\partial a}y_{t-1}\right] \quad (38)$$

$$+ \delta n_{in}\text{Max}\left[w_{in}\sigma'_{in}\frac{\partial}{\partial a}y_{t-1}^{in}\right] - \text{Min}\left[thr\sigma'\frac{\partial}{\partial a}y_{t-1}\right] \quad (39)$$

$$= \text{Max}\left[\alpha_{decay}\right]\text{Max}\left[\frac{\partial}{\partial a}y_{t-1}\right] + (n_{rec} - 1)\text{Max}\left[w_{rec}\right]\text{Max}\left[\sigma'\right]\text{Max}\left[\frac{\partial}{\partial a}y_{t-1}\right] \\ + \delta n_{in}\text{Max}\left[w_{in}\right]\text{Max}\left[\sigma'_{in}\right]\text{Max}\left[\frac{\partial}{\partial a}y_{t-1}^{in}\right] - \text{Max}\left[thr\right]\text{Max}\left[\sigma'\right]\text{Min}\left[\frac{\partial}{\partial a}y_{t-1}\right] \quad (40)$$

$$= \text{Max}\left[\alpha_{decay}\right]\text{Max}\left[\frac{\partial}{\partial a}y_{t-1}\right] + (n_{rec} - 1)\text{Max}\left[w_{rec}\right]\gamma\text{Max}\left[\frac{\partial}{\partial a}y_{t-1}\right] \\ + n_{in}\delta\text{Max}\left[w_{in}\right]\gamma_{in}\text{Max}\left[\frac{\partial}{\partial a}y_{t-1}^{in}\right] - \text{Max}\left[thr\right]\gamma\frac{\text{Max}\left[w_{rec}\right]}{\text{Min}\left[w_{rec}\right]}\text{Max}\left[\frac{\partial}{\partial a}y_{t-1}\right] \quad (41)$$

where we used the fact that σ' and thr are positive in the second equality, and we assumed that $\text{Max}\left[w_{rec}\right]\text{Max}\left[\frac{\partial}{\partial a}y_{t-1}\right] = \text{Min}\left[w_{rec}\right]\text{Min}\left[\frac{\partial}{\partial a}y_{t-1}\right]$ in the third equality, which for symmetrical weight initialization simply means that $\text{Max}\left[\frac{\partial}{\partial a}y_{t-1}\right] = -\text{Min}\left[\frac{\partial}{\partial a}y_{t-1}\right]$. We apply condition III, which states that all maximal gradients are equivalent, so, they can be cancelled out, and we have

$$1 = \text{Max}\left[\alpha_{decay}\right] + (n_{rec} - 1)\text{Max}\left[w_{rec}\right]\gamma + \delta n_{in}\text{Max}\left[w_{in}\right]\gamma_{in} - \text{Max}\left[thr\right]\gamma\frac{\text{Max}\left[w_{rec}\right]}{\text{Min}\left[w_{rec}\right]} \quad (42)$$

$$1 = \text{Max}\left[\alpha_{decay}\right] + \delta n_{in}\text{Max}\left[w_{in}\right]\gamma_{in} + \gamma\text{Max}\left[w_{rec}\right]\frac{(n_{rec} - 1)\text{Min}\left[w_{rec}\right] - \text{Max}\left[thr\right]}{\text{Min}\left[w_{rec}\right]} \quad (43)$$

$$\gamma = \frac{\text{Min}\left[w_{rec}\right]}{(n_{rec} - 1)\text{Min}\left[w_{rec}\right] - \text{Max}\left[thr\right]}\frac{1}{\text{Max}\left[w_{rec}\right]}\left(1 - \text{Max}\left[\alpha_{decay}\right] - \delta \cdot n_{in}\text{Max}\left[W_{in}\right]\gamma_{in}\right) \quad (44)$$

where we only had to rearrange terms. This final equation gives the value that the dampening has to take to make condition III true at initialization.

B.4 Impact on the SG second moment of backward pass variance stability (Condition IV)

We apply condition IV to the LIF network to constrain the choice of surrogate gradient variance. Condition IV states that we want the variance of the gradient to remain stable across time and layers. Taking the derivative of the LIF and followed by the variance

$$\frac{\partial}{\partial a}y_t = \alpha_{decay}\frac{\partial}{\partial a}y_{t-1} + W_{rec}\sigma'\frac{\partial}{\partial a}y_{t-1} + W_{in}\frac{\partial}{\partial a}z_t - thr\sigma'\frac{\partial}{\partial a}y_{t-1} \quad (45)$$

$$\frac{\partial}{\partial a}y_t = \alpha_{decay}\frac{\partial}{\partial a}y_{t-1} + W_{rec}\sigma'\frac{\partial}{\partial a}y_{t-1} + \xi W_{in}\sigma'_{in}\frac{\partial}{\partial a}y_{t-1}^{in} - thr\sigma'\frac{\partial}{\partial a}y_{t-1} \quad (46)$$

$$\text{Var}\left[\frac{\partial}{\partial a}y_t\right] = \text{Var}\left[\alpha_{decay}\frac{\partial}{\partial a}y_{t-1}\right] + \text{Var}\left[W_{rec}\sigma'\frac{\partial}{\partial a}y_{t-1}\right] \\ + \text{Var}\left[\xi W_{in}\sigma'_{in}\frac{\partial}{\partial a}y_{t-1}^{in}\right] + \text{Var}\left[thr\sigma'\frac{\partial}{\partial a}y_{t-1}\right] \quad (47)$$

$$\text{Var}\left[\frac{\partial}{\partial a}y_t\right] = \text{Var}\left[\alpha_{decay}\frac{\partial}{\partial a}y_{t-1}\right] + (n_{rec} - 1)\text{Var}\left[w_{rec}\sigma'\frac{\partial}{\partial a}y_{t-1}\right] \\ + n_{in}\text{Var}\left[\xi w_{in}\sigma'_{in}\frac{\partial}{\partial a}y_{t-1}^{in}\right] + \text{Var}\left[thr\sigma'\frac{\partial}{\partial a}y_{t-1}\right] \quad (48)$$

where $\xi = 0$ if z_t represents the data and $\xi = 1$ if it represents the layer below in the stack. We denote by σ'_{in} the surrogate gradient of the layer below.

Assuming gradients with mean zero,

$$\text{Var}[wg] = (\text{Var}[g] + E[g]^2)(\text{Var}[w] + E[w]^2) - E[g]^2 E[w]^2 \quad (49)$$

$$= E[g^2]E[w^2] - E[g]^2 E[w]^2 \quad (50)$$

$$= \text{Var}[g](\text{Var}[w] + E[w]^2) \quad (51)$$

$$= \text{Var}[g]E[w^2] \quad (52)$$

which gives

$$\text{Var}\left[\frac{\partial}{\partial a} y_t\right] = E[\alpha_{decay}^2] \text{Var}\left[\frac{\partial}{\partial a} y_{t-1}\right] + (n_{rec} - 1)E[(w_{rec}\sigma')^2] \text{Var}\left[\frac{\partial}{\partial a} y_{t-1}\right] \quad (53)$$

$$+ \xi \cdot n_{in} E[(w_{in}\sigma'_{in})^2] \text{Var}\left[\frac{\partial}{\partial a} y_{t-1}^{in}\right] + E[(thr\sigma')^2] \text{Var}\left[\frac{\partial}{\partial a} y_{t-1}\right] \quad (54)$$

We apply condition IV, we want gradients to have the same variance, irrespective of the time step, or the neuron in the stack, so we cancel them out, which results in

$$1 = E[\alpha_{decay}^2] + (n_{rec} - 1)E[(w_{rec}\sigma')^2] + \xi \cdot n_{in} E[(w_{in}\sigma'_{in})^2] + E[(thr\sigma')^2] \quad (55)$$

$$1 = E[\alpha_{decay}^2] + (n_{rec} - 1)E[w_{rec}^2]E[\sigma'^2] + \xi \cdot n_{in} E[w_{in}^2]E[\sigma'_{in}^2] + E[thr^2]E[\sigma'^2] \quad (56)$$

where we used the fact that for independent variables X, Y we have $E[X^p Y^q] = E[X^p]E[Y^q]$ in the third line. Therefore the implied condition on the SG is

$$E[\sigma'^2] = \frac{1 - E[\alpha_{decay}^2] - \xi \cdot n_{in} E[w_{in}^2]E[\sigma'_{in}^2]}{(n_{rec} - 1)E[w_{rec}^2] + E[thr^2]} \quad (57)$$

This is the value to pick for the second non-centered moment of the SG, if we want condition IV to hold.

B.5 Applying Condition IV to the exponential SG

We show how we apply equation 57, to choose the sharpness of an exponential SG. For that we need to define the dependence of the variance of the SG with its sharpness. We use as equivalent notation for the surrogate gradient

$$\delta\tilde{H} = \sigma' = \frac{\partial\tilde{H}}{\partial v} = \gamma f(s \cdot v)$$

The moments of the surrogate gradient are given by

$$E[\delta\tilde{H}^m] = \int \delta\tilde{H}^m p(\delta\tilde{H}) d\delta\tilde{H} \quad (58)$$

$$= \iint \delta\tilde{H}^m p(\delta\tilde{H}|v) p(v) dv d\delta\tilde{H} \quad (\text{marginalization}) \quad (59)$$

$$= \iint \delta\tilde{H}^m \delta(\delta\tilde{H} - \delta\tilde{H}(v)) d\delta\tilde{H} p(v) dv \quad (\delta\tilde{H} \text{ is deterministic on } v) \quad (60)$$

$$= \int \delta\tilde{H}(v)^m p(v) dv \quad (61)$$

where $v = y - thr$. We are going to assume as the non-informative prior a uniform distribution between the minimal and maximal values of $y_t - thr$.

$$E[\delta\tilde{H}(v)^m] = \int \delta\tilde{H}(v)^m p(v) dv \quad (62)$$

$$= \frac{1}{y_{max} - y_{min}} \int_{y_{min}-thr}^{y_{max}-thr} \delta\tilde{H}(v)^m dv \quad (\text{non informative prior}) \quad (63)$$

$$= \frac{\gamma^m}{s(y_{max} - y_{min})} \int_{s(y_{min}-thr)}^{s(y_{max}-thr)} f(v')^m dv' \quad (\text{SG definition and } v' = sv) \quad (64)$$

Considering the exponential SG we have that

$$\int_{v_-}^{v_+} \text{exponential}(v)^m dv = \int_{v_-}^{v_+} e^{-2m|v|} dv \quad (65)$$

$$= \int_0^{|v_+|} e^{-2mv} dv + \int_0^{|v_-|} e^{-2mv} dv \quad (66)$$

$$= -\frac{1}{2m} e^{-2m|v_+|} - \frac{1}{2m} e^{-2m|v_-|} + 2\frac{1}{2m} \quad (67)$$

and we show how to compute $y_{max} = \text{Max}[y_t]$ and $y_{min} = \text{Min}[y_t]$ in section B.6. Since the dependence with s is quite complex, we find the s that satisfies the last equation and equation 57 through random search, where $E[\delta\tilde{H}(v)^2] = E[\sigma'(v)^2]$. This is how condition IV is used to fix the sharpness of an SG.

B.6 Maximal and Minimal voltage values achievable by the network at initialization

We calculate the maximum and minimum value that the voltage y can take, to be able to complete the argument about the variance of the backward pass of section B.5. First, we use Min and Max in a statistical ensemble sense, as the maximum/minimum value that a variable could take if sampled over and over again

$$\text{Max}[X] = \sup_{x \sim p(x)} x \quad (68)$$

$$\text{Min}[X] = \inf_{x \sim p(x)} x \quad (69)$$

when applied to the definition of LIF

$$\text{Max}[y_t] = \text{Max}[\alpha_{decay} y_{t-1}] + \text{Max}[W_{rec} x_{t-1}] + \text{Max}[b] + \text{Max}[W_{in} z_t] - \text{Min}[thr x_{t-1}] \quad (70)$$

$$= \text{Max}[\alpha_{decay}] \text{Max}[y_{t-1}] + (n_{rec} - 1) \text{Max}[w_{rec}] + \text{Max}[b] + n_{in} \text{Max}[w_{in}] - \text{Max}[thr] \text{Min}[x_{t-1}] \quad (71)$$

$$\text{Max}[y_t] = \frac{1}{1 - \text{Max}[\alpha_{decay}]} \left((n_{rec} - 1) \text{Max}[w_{rec}] + \text{Max}[b] + n_{in} \text{Max}[w_{in}] \right) \quad (72)$$

where we used the fact that if x_t, z_t were sampled over and over, the maximum value that they could take is all neurons having fired at the same time, while the minimum would be achieved when all the neurons in the layer would stay silent, we used the fact that $\alpha_{decay}, thr > 0$, and we assumed that the maximum is going to stay constant through time $\text{Max}[y_{t-1}] = \text{Max}[y_t]$. Notice that the maximal voltage is achieved when all the neurons in the layer fired at $t - 1$, equation 71, except for the neuron under study, that stayed silent at $t - 1$, to have 72. Similarly for the bound to the minimal voltage:

$$\begin{aligned} \text{Min}[y_t] &= \text{Min}[\alpha_{decay}y_{t-1}] + (n_{rec} - 1)\text{Min}[w_{rec}x_{t-1}] + \text{Min}[b] + n_{in}\text{Min}[w_{in}z_t] - \text{Max}[thr\ x_{t-1}] \\ & \tag{73} \end{aligned}$$

$$= \text{Max}[\alpha_{decay}]\text{Min}[y_{t-1}] + (n_{rec} - 1)\text{Min}[w_{rec}] + \text{Min}[b] + n_{in}\text{Min}[w_{in}] - \text{Max}[thr] \tag{74}$$

$$\text{Min}[y_t] = \frac{1}{1 - \text{Max}[\alpha_{decay}]} \left((n_{rec} - 1)\text{Min}[w_{rec}] + \text{Min}[b] + n_{in}\text{Min}[w_{in}] - \text{Max}[thr] \right) \tag{75}$$

Second, we consider another definition of *Min* and *Max*, where we consider the maximum value achievable by the current sample from the weight distribution. The real maximum value of the voltage will be achieved when the presynaptic neurons to fire are those that are connected with positive weight, we then have that our equation turns to

$$\text{Max}[y_t]_i = \alpha_{decay,i}\text{Max}[y_{t-1}]_i + \sum_j \text{ReLU}[W_{rec}]_{ij} + b_i + \sum_j \text{ReLU}[W_{in}]_{ij} - \text{Min}[thr\ x_{t-1}]_i \tag{76}$$

$$\text{Max}[y_t]_i = \frac{1}{1 - \alpha_{decay,i}} \left(\sum_j \text{ReLU}[W_{rec}]_{ij} + b_i + \sum_j \text{ReLU}[W_{in}]_{ij} \right) \tag{77}$$

where we refer as $\sum_j \text{ReLU}[W_{rec}]_{ij}$ the sum over columns, where we have typically omitted the index i for the element of the vector for cleanliness in the rest of the article. The case for the minimum is analogous

$$\text{Min}[y_t]_i = \alpha_{decay,i}\text{Min}[y_{t-1}]_i + \text{Min}[W_{rec}x_{t-1}] + b_i + \text{Min}[W_{in}z_t] - \text{Max}[thr\ x_{t-1}] \tag{78}$$

$$\text{Min}[y_t]_i = \frac{1}{1 - \alpha_{decay,i}} \left(- \sum_j \text{ReLU}[-W_{rec}]_{ij} + b_i - \sum_j \text{ReLU}[-W_{in}]_{ij} - thr_i \right) \tag{79}$$

With this we showed how we calculated the maximal and minimal value of the voltage, to be able to use condition IV to define the sharpness of the SG in section B.5.

B.7 Applying conditions I-IV to an alternative definition of reset

We want to show how the constraints on the weights initialization and on the SG choice change, when the neuron model definition changes. SNU [Woźniak et al., 2020] uses a LIF with a different definition of reset, that we will call multiplicative reset

$$y_t = \alpha_{decay}(y_{t-1} + i_t)(1 - x_t) \tag{80}$$

$$i_t = W_{rec}x_t + W_{in}z_t + b \tag{81}$$

This definitions performs as well one refractory period, while if defined like $y_t = \alpha_{decay}y_{t-1}(1 - x_t) + i_t$, would not result in a y_t clamped to zero when $x_t = 1$. The factor $(1 - x_t)$ takes the voltage exactly to zero every time the neuron has fired, zero being the equilibrium voltage. What is interesting about this form of reset is that the voltage is reset exactly to $y = 0$ after firing, while with the subtractive reset it is not the case. In our experience both resets gave similar performance. We can retrieve the new initializations from the ones corresponding to the additive reset by observing that we only have to change $\alpha_{decay} \rightarrow \alpha_{decay}(1 - x_t)$ and removing the previously used subtractive reset. The equations that result from the 4 desiderata for this neuron definition, LIF with multiplicative reset, are as follows

$$Mean[w_{rec}] = \frac{1}{n_{rec} - 1} \left(1 - Mean[\alpha_{decay}] \right) Mean[thr] \quad \text{CI} \quad (82)$$

$$Var[w_{rec}] = 2(Var[z_t] + Mean[z_t]^2) \frac{n_{in}}{n_{rec} - 1} Var[w_{in}] - \frac{1}{2} Mean[w_{rec}]^2 \quad \text{CII} \quad (83)$$

$$\gamma = \frac{1}{(n_{rec} - 1) Max[w_{rec}]} \left(1 - \alpha_{decay} - \xi n_{in} Max[w_{in}] \gamma_{in} \right) \quad \text{CIII} \quad (84)$$

$$E[\sigma'^2] = \frac{1 - E[\alpha_{decay}^2]/2 - \xi n_{in} E[w_{in}^2] E[\sigma_{in}'^2]}{(n_{rec} - 1) E[w_{rec}^2]} \quad \text{CIV} \quad (85)$$